Advances in Nano Research, *Vol. 13, No.4 (2022) 325-339*
https://doi.org/10.12989/anr.2022.13.4.325

Prospecting endophytic colonization in *Waltheria indica* for biosynthesis of silver nanoparticles and its antimicrobial activity

C.Nirmala and M.Sridevi*

Department of Biotechnology, Vinayaka Mission's Kirupananda Variyar Engineering College, Vinayaka Mission's Research Foundation (Deemed to be University), Salem, Tamilnadu, India

(*Received October 4, 2020, Revised July 28, 2022, Accepted July 29, 2022*)

Abstract. Endophytes ascertain a symbiotic relationship with plants as promoters of growth, defense mechanism etc. This study is a first report to screen the endophytic population in *Waltheria indica*, a tropical medicinal plant. 5 bacterial and 3 fungal strains in leaves, 3 bacterial and 1 yeast species in stems were differentiated morphologically and identified by biochemical and molecular methods. The phylogenetic tree of the isolated endophytes was constructed using MEGA X. Silver nanoparticles were biosynthesized from a rare endophytic bacterium *Cupriavidus metallidu*rans isolated from the leaf of *W. indica*. The formation of silver nanoparticles was confirmed by UV-Visible spectrophotometer that evidenced a strong absorption band at 408.5 nm of UV-Visible range with crystalline nature and average particle size of 16.4 nm by Particle size analyzer. The Fourier Transform Infra-Red spectrum displayed the presence of various functional groups that stabilized the nanoparticles. X-ray diffraction peaks were conferred to face centered cubic structure. Transmission Electron Microscope and Scanning Electron Microscope revealed the spherical-shaped, polycrystalline nature with the presence of elemental silver analyzed by Energy Dispersive of X-Ray spectrum. Selected area electron diffraction also confirmed the orientation of AgNPs at 111, 200, 220, 311 planes similar to X-ray diffraction analysis. The synthesized nanoparticles are evaluated for antimicrobial activity against 7 bacterial and 3 fungal pathogens. A good zone of inhibition was observed against pathogenic bacteria than fungal pathogens. Thus the study could hold a key aspect in drug discovery research and other pharmacological conducts of human clinical conditions.

Keywords: antimicrobial activity; *Cupriavidus metallidurans*; endophytes; silver nanoparticles; *Waltheria indica*

1. Introduction

Every plant species from lower forms like mosses to higher-order trees are the natural host for microorganisms. They colonises the tissues externally, internally and imparts both beneficial and harmful effects to the plants. Endophytic microorganisms harboured from internal layers of medicinal plants are important sources of novel products for drug discovery, industrial and agricultural applications (Zhang *et al*. 2006). They diversify with plants, species, regions, climatic changes (Nair and Padmavathy 2014) and confer major ecological benefits to their host plants. The advent of unusual strides of endophytes, their importance in influencing the plant growth, the ability of a plant to resist infection, stress conditions and other insights sparked a huge interest in their exploration. Traditionally, plants are considered as potential sources for novel bioactive moieties (Chockalingam and Muruhan 2017) that may be the products of the plant itself or the endophytes residing inside the tissues. *Waltheria indica*, a tropical perennial medicinal plant of Sterculiaceae family is used in traditional medicine by different communal worldwide (Zongo *et al*. 2013, Nirmala and Sridevi 2021). The plant is extensively screened for the phytochemicals and their related pharmacological properties (Kannan *et al*. 2016, Monteillier *et al*. 2017, Zailani *et al*. 2010). Yet the endophytic association in that plant is not explored, which is a promising area of development for novel bioactive compounds.

Nanoscience, an advanced interdisciplinary research field deals with synthesis of nanomaterials with unique catalytic, magnetic and electrical properties. Nanostructures of various composite formulations with controlled shape and size is designed for diverse applications. They are used as sorbents in waste water treatment (Yildiz *et al*. 2017), as catalysts for dehydrogenation reaction (Sen *et al*. 2018), for Selective reduction of nitro compounds in heterogeneous reactions (Göksu *et al*. 2016, 2017), as conductive conduit in thermopower generations (Abrahamson 2013) etc. Physical techniques such as optical lithography, use of electron beams, ion beams, anisotropic dissolution, thermal decomposition, templated etching, and selective dealloying are practiced for the nanoparticles (NPs) synthesis (Iqbal *et al*. 2012). In chemical methods inorganic and organic solvents are used to reduce the chemical species into NPs. Though defined structured, stable NPs are produced by physicochemical processes they are time consuming, requires high energy, highly toxic and also lead to nano contamination in the environment (Deepak *et al*. 2019).

The merge of biology with nanotechnology lead to the focus on the use of bio sources such as microbes, plants, and their biomolecules for the synthesis of metal NPs. The approach was proved to be economical, safe, resource efficient and greener alternative (Mariadoss *et al*. 2019) for physical and chemical techniques. The compounds in the plant extracts such as saponins, alkaloids, terpenoids

*Corresponding author, Ph.D.,
E-mail: drsridevimuruhan@gmail.com

ISSN: 2287-237X (Print), 2287-2388 (Online)

flavonoids, quinines, phenols, sulfhydryls, pigments, tannins, sugars, and microbial metabolites such as enzymes, aminoacids, proteins, alcoholic compounds and vitamins fabricates the NPs with enhanced stability, increased inhibitory and cellular toxicity characteristics. At this juncture endophyte-mediated biosynthesis of NPs has emerged as the latest research prospect (Rahman *et al*. 2019). The fastidious growth of endophytes, presence of valuable, novel extracellular and intracellular metabolites and ease of maintenance gained more importance for the synthesis of stable NPs for biomedical and pharmaceutical applications (Singh *et al*. 2014). Comparatively, extracellular synthesis of NPs is simple, and cost effective than intracellular methods that require additional process to purify the synthesized NPs. The applications oriented customization of size and shape raised the demand for biosynthesised silver NPs (AgNPs) than the other metallic NPs (Diantoro *et al*. 2018). Their distinctive surface chemistry, broad-spectrum antimicrobial activity, low toxicity, increase solubility and enhanced bioavailability in disease treatment augmented its importance in the development of drug formulations. The wide range biological activity exhibited by AgNPs hold forth the applications in veterinary, plant science, environmental concerns and electronics (Nirmala and Sridevi 2021).

Based on the above literature survey, in the present study the diversity of endophytic groups in the stem and leaf parts of *W. indica* are identified and explored for the first time. The bacterial strain *Cupriavidus sp*. so for isolated from environmental samples, legumes is uniquely identified in the leaves of *W. indica*. Due to its potential metal resistance property it is employed for AgNPs synthesis. The optimal formation of NPs is ensured by various characterisation studies and its antimicrobial activity was evaluated *in vitro*. Hence a greener approach for NPs synthesis and production of targeted nanomaterials at very high efficiency in pharmaceutical preparations is proposed to unveil the role of endophytes in biomedical applications.

2. Materials and methods

2.1 Plant materials

Healthy plant samples of *W. indica*, were collected freshly near foothills of Kanjamalai, Salem (Latitude: 11° 36' 59" N, Longitude: 78° 3' 32" E) and transported to the laboratory in pre-sterilised zip-lock poly bags. These samples were washed in running tap water to remove soil particles, adhered debris and finally washed with distilled water. The collected plant material was authenticated at Botanical Survey of India, Southern Regional Centre, Coimbatore with identification No. BSI/SRC/5/23/2020/ TECH/562. The disease-free inner layers of leaf blade and stem were used for further isolation of endophytes (Fig. 1).

2.2 Sample preparation

The leaf and stem parts of the plant collected within 24 hours are surface sterilized with 70% ethanol for 10 minutes, 4% sodium hypochlorite for 1.5 minutes, and 70% ethanol again for l minute followed by five times rinses in sterile distilled water. Samples were cut aseptically using the sterile knife and inner tissues were excised, rinsed three times with sterile distilled water and dried on sterile blotting paper.

Fig. 1 *Waltheria indica*

2.3 Endophytes isolation and cultivation

1 gram of inner tissues of leaf and stem were segmented into small pieces, macerated separately in 0.89 % saline and diluted tenfold in sterile saline. 0.1ml of serial diluted tissue extracts ($10^{-1}$and 10^{-2}) were spread on nutrient agar (NA) and potato dextrose agar (PDA) incubated at 37°C for 48 to 72 hours and 5-6 days at 30°C for bacterial and fungal isolation respectively. The plating was done in triplicate for each dilution. Bacterial colonies were differentiated based on their time of growth and morphology (colony color, size, and shape) and purified by streaking techniques in agar slants. The hyphal tips appeared in PDA were carefully pure cultured and incubated at 28°C for two weeks (Correll *et al*. 1987). To confirm the effectiveness of disinfestations of samples, sterility checks were carried out by taking sample impressions (0.1 ml of the final rinse water plated on NA and PDA) and incubated for about 6 days as control plates. The absence of microbial growth in control plates confirms that the sample was sterile and microbes isolated were endophytes (Qin *et al*. 2009). The purified cultures were further characterized by biochemical and molecular methods.

2.4 Identification of endophytes

2.4.1 Phenotypic identification of endophytes

The obtained endophytic colonies were coded according to their source tissues as Endophytic Bacteria Leaf (EBL) EBL1, EBL2 etc., Endophytic Bacteria Stem (EBS) EBS1, EBS2 etc., Endophytic Fungi Leaf (EFL) EFL1, EFL2, etc., and Endophytic Fungi Stem (EFS) EFS1, EFS2 etc. The different morphospecies of bacteria were selected, identified by colony shape, size and colour and biochemically analyzed by Gram staining, motility, spore

staining, IMViC, TSI, Starch Hydrolysis, Carbohydrates, Oxidase, and Catalase test based on Bergey's Manual of Determinative Bacteriology (Buchanan and Gibbons 1975). The fungal endophytes were identified morphologically by colony characteristics, color (front and reverse), growth, structure and morphology of conidiophores and conidia by lactophenol cotton blue staining method. The Urease test is performed for yeast. The obtained taxa were compared with the descriptions of fungal species (Barnett and Hunter 1998).

2.4.2 DNA Extraction and PCR amplification of endophytes

The 16S rRNA gene of bacteria (EBL1, EBL3, EBL4, EBL6, EBL9, EBS2, EBS3, and EBS5) is the molecular signatures for bacterial identification to species level. The DNA was isolated by using High pure PCR template preparation kit, Roche. The 1500 bp of 16S rRNA genes are amplified using bacterial specific PCR primers, forward primer 27F (5'AGAGTTTGATCMTGGCTCAG3'), 1492R (5'TACGGYTACCTTGTTACGACTT3') (Frank *et al*. 2008). Molecular identification of endophytic fungi and yeast (EFL1, EFL2, EFL3 and ESF1) were carried out by 18S rDNA gene sequence. After seven days of fungal growth, the genomic DNA of each isolate were extracted using High pure PCR template kit, Roche and 18S rDNA gene was amplified with universal primers UL18F (5'TGTACACACCGCCCGTC3'), and UL28R (5'ATCGC CAGTTCTGCTTAC3') (Martin and Rygiewicz 2005, White *et al*. 1990) by polymerase chain reaction (PCR) (Veriti^{TM}-96 Well Thermocycler). The PCR reaction mixture contained Double distilled water (18.3 µl), Taq DNA polymerase buffer (10x - 2.5 µl), dNTP mix (2mM - 2.5 µl), Forward Primers (10µM - 0.5 µl), Reverse Primers (10µM - 0.5 µl), Template DNA (0.5 µl), and Taq DNA polymerase enzyme (5U/µl - 0.2 µl). The thermo cycler was programmed with initial denaturation at 94°C for 5 minutes, Annealing at 55°C for 45 seconds, Extension at 72°C for 1 minute and final extension at 72°C for 5 minutes (Saravanakumar *et al*. 2021). The obtained PCR products were separated in 1.5 % agarose gel in TAE buffer and the DNA bands obtained are eluted by MACHEREY- NAGEL PCR clean up kit. Sequencing was done by Sanger dideoxy sequencing method (Applied Biosystems, Thermofisher Scientific).

2.4.3 Sequence alignment and phylogenetic analysis

The sequences obtained are run through multiple BLASTn in NCBI GenBank database (Altschul *et al*. 1990) to identify the homologous sequences. The identical hits obtained are selected, downloaded and aligned using MUSCLE by UPGMA clustering method in MEGA X software program (Kumar *et al*. 2018). The evolutionary history was inferred using the Neighbor-Joining method (Saitou and Nei 1987) with bootstrap consensus tree inferred from 1000 replicates. Branches analogous to partitions less than 50% bootstrap replicates are distorted. Next to the branches, the percentage of replicate trees in which the associated taxa clustered together in the bootstrap test (1000 replicates) is shown (Felsenstein 1985). The phylogenetic distances between the isolates were assessed using the Maximum Composite Likelihood method (Tamura *et al*. 2004) and the uncertain positions for each sequence were removed by pairwise deletion.

2.5 Biosynthesis of silver nanoparticles

The isolated endophytic bacterial strain *Cupriavidus metallidurans* (*Cm*) was cultured in 100ml of Luria–Bertani medium and incubated on an orbital shaker at 37°C and agitated at 200 rpm for 24 hours. The biomass was harvested by centrifuging at 10000 rpm for 10 minutes. 10 ml of bacterial supernatant was mixed with 90ml (1mM) silver nitrate ($AgNO_3$) solution for the biosynthesis of AgNPs. A positive control of the supernatant in deionised water without $AgNO_3$ was also maintained. The prepared solutions were incubated at 30°C for 24 hours in dark to avoid any photochemical reactions. The biosynthesized silver nanoparticles (*Cm*-AgNPs) were purified by centrifugation at 10,000 rpm for 5 minutes twice, and freeze-dried. The sample was resuspended in deionized water for further characterization studies

2.6 Characterization studies for silver nanoparticles

The absorption spectrum of *Cm*-AgNPs was determined using UV-Visible spectroscopy (SHIMADZU 1800) in 200–600 nm range with medium scanning speed of 300 nm min^{-1}. The particle size and distribution pattern of *Cm*-AgNPs were evaluated by dynamic light scattering analysis (DLS) and the electrophoretic stability were determined by the Zeta potential analysis using zeta sizer (Malvern instruments Ltd., U.K ZS90). The FTIR spectra of *Cm*-AgNPs is measured at a resolution of 1 cm^{-1} in the transmission mode from wave numbers 500 to 4000 cm^{-1} in solid phase using SHIMADZU, IR PRESTIGE 21. The FTIR spectrum determines the potential biomolecules in the bacterial extract responsible for the reduction and capping of nanoparticles. The structure and composition of *Cm*-AgNPs were analyzed by XRD (SHIMADZU - XRD 6000) operated at a voltage of 40kV and a current of 30mA equipped with a proportional counter Cu Kα radiation in a θ-2θ scanning mode between 10 to 80 degrees with sampling pitch of 0.1000 degree. The crystallite domain sizes were calculated from the width of the XRD peaks using Debye-Scherrer formula (Cullity 1978) $D = 0.94\lambda/\beta\cos\theta$, where D is the average crystallite domain size perpendicular to the reflecting planes, λ is the X-ray wavelength, β is the full width at half maximum (FWHM), and θ is the diffraction angle. The size and surface morphological properties of *Cm*-AgNPs were determined by Transmission Electron Microscope (TEM) (JEOL JEM 2100) and selected area electron diffraction (SAED) pattern was obtained. The sample was located on copper grids coated carbon films, dried at room temperature and analyzed at 200kV. Scanning Electron Microscopic (SEM) (JEOL– JSM 6390) at a voltage of 15–20kV at different magnifications was also used to measure the crystallite structure of the *Cm*-AgNPs. The atomic composition of *Cm*-AgNPs was confirmed by energy-dispersive X-ray (EDX) analysis (Oxford instrument, INCA PentaFET x3) coupled with SEM.

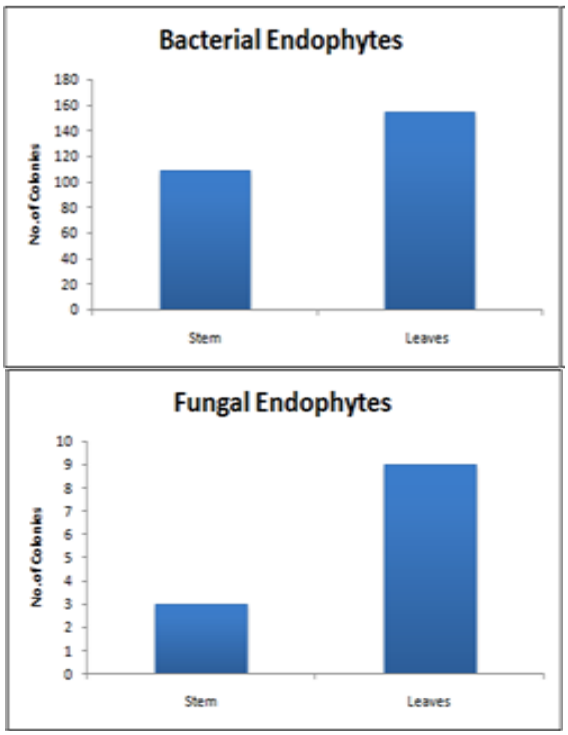

Fig. 2 Endophytic population from *W. indica* stems and leaves

2.7 Screening of antimicrobial activity of silver nanoparticles

2.7.1 Test organisms

The bioactivity of *Cm*-AgNPs synthesized from endophytic extract was analyzed by antimicrobial assay against bacterial and fungal pathogenic cultures obtained from Microbial Type Culture Collection (MTCC), Chandigarh. The test organisms include Gram positive bacteria *Bacillus subtilis* (MTCC1133), *Staphylococcus aureus* (MTCC2940), *Staphylococcus epidermidis* (MTCC737), Gram negative *Escherichia coli* (MTCC40), *Klebsiella pneumonia* (MTCC2405), *Proteus mirabilis* (MTCC425), *Salmonella typhi* (MTCC733) and fungal strains of *Penicillium chrysogenum* (MTCC947), *Candida albicans* (MTCC183) and *Aspergillus niger* (MTCC404).

2.7.2 Antimicrobial activity

Agar well diffusion method was done to determine the antimicrobial activity of the synthesized *Cm*-AgNPs. The test bacterial culture in exponential growth phase grown in nutrient broth was swabbed in Muller Hinton agar plates and fungal culture onto the surface of PDA. Agar wells of 5 mm diameter were prepared using a cork borer. The *Cm*-AgNPs dissolved in dimethyl sulfoxide (DMSO) in different concentration (25µg/mL, 50µg/mL, 75µg/mL, 100µg/mL) were added to the wells. DMSO (10µg/mL) as a negative control, Tetracycline (10µg/mL) and Kanamycin (10µg/mL) as positive control were maintained in parallel for bacterial and fungal pathogens respectively and incubated at 37°C for 24 hours. Clear zones of inhibition were observed and the diameter of such zones are measured and recorded.

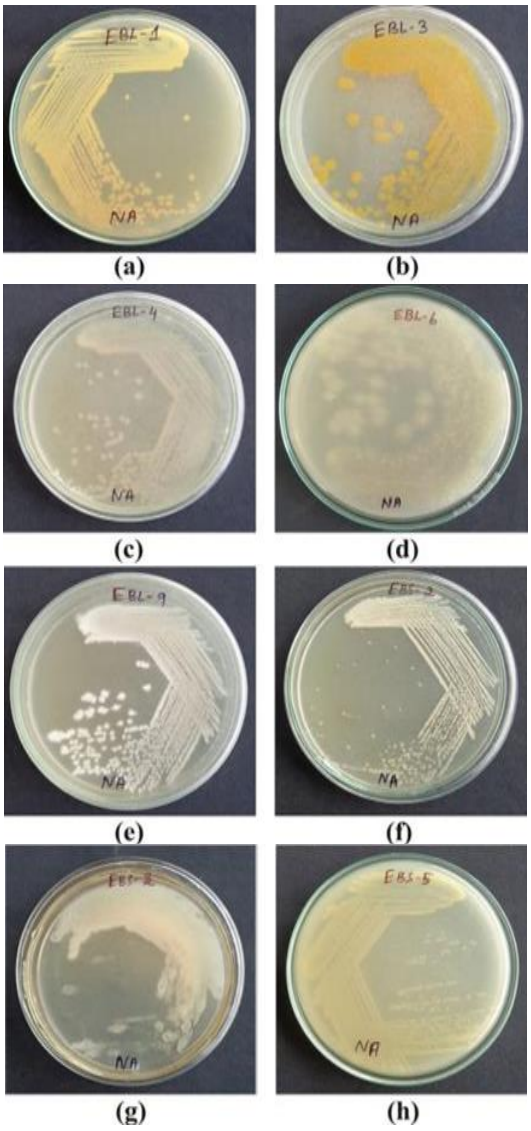

Fig. 3 Bacterial endophytes (a) EBL1 (b) EBL3 (c) EBL4 (d) EBL6 (e) EBL9 (f) EBS2 (g) EBS3 (h) EBS5

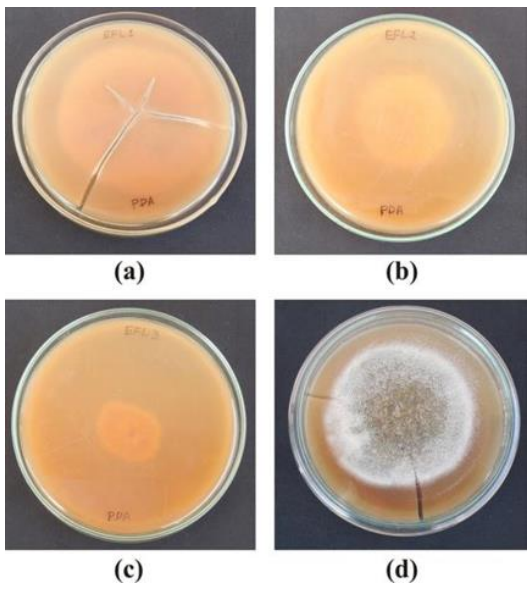

Fig. 4 Fungal endophytes endophytes (a) EFL1 (b) EFL2 (c) EFL3 (d) EFS3

Table 1 Phenotypic identification of bacterial endophytes

Biochemical Parameters		Bacterial endophytes							
		EBL1	EBL3	EBL4	EBL6	EBL9	EBS2	EBS3	EBS5
Colony Morphology	Colour	Yellow	Yellow	Creamy White	White	Milky White	Light Yellow	Pale White	Yellow
	Shape	Round	Irregular	Round	Irregular	Irregular	Irregular	Irregular	Round
	Opacity	Opaque	Opaque	Opaque	Transparent	Opaque	Opaque	Transparent	Opaque
Gram staining		+	+	+	+	+	+	+	-
Cell morphology		Cocci	Rod	Rod	Rod	Cocci	Rod	Rod	Rod
Motility		+	+	-	+	+	+	+	+
Spore staining		-	-	-	-	-	-	-	-
IMViC	Indole	-	+	+	-	-	-	-	-
	MR	-	+	+	-	-	-	-	-
	VP	-	-	+	+	+	+	+	-
	Citrate	-	-	+	+	-	-	+	+
TSI	Butt	A	A	A	A	A	A	A	A
	Slant	A	K	K	K	K	K	A	K
	H_2S Production	-	-	-	-	-	-	-	-
	Gas production	-	-	-	-	-	-	-	-
Starch Hydrolysis		-	+	-	+	-	-	+	-
Carbohydrates	Glucose	+	-	-	+	+	+	+	+
	Lactose	-	-	+	+	+	-	+	+
	Maltose	+	-	-	-	+	-	+	-
	Mannitol	+	-	-	-	-	-	+	-
	Sucrose	+	-	-	-	+	+	+	-
Oxidase		+	+	+	+	-	+	-	-
Catalase		+	+	+	+	+	-	+	+

3. Results and discussion

3.1 Endophytic population

The control plates showed no microbial growth thus confirmed the microbes grown in NA and PDA are endophytes. A total of 276 colonies that included 264 bacterial endophytes and 12 fungal endophytes were obtained correspondingly from stem and leaves of *W. indica*. Of these detected 264 bacterial endophytes, 109 (41.28%) counts from stem and 155 (58.71%) from leaves were observed. Among 12 fungal endophytes, 3 (25%) colonies were from stem and 9 colonies (75%) from leaves (Fig. 2). The leaf supported significantly higher counts of bacterial and fungal endophytes compared to stem that confirms the distribution of endophytes varies among the plant tissues. This may be due to the presence of various phytochemicals constituted in leafs than the other parts of the plant (Nirmala and Sridevi 2021).

3.2 Identification of endophytes

3.2.1 Phenotypic identification of endophytes

Similar morphological features were observed in many isolates. Hence based on the macroscopic features 5different bacterial colonies from leaves (EBL1, EBL3, EBL4, EBL6, EBL9), 3 bacterial colonies from stems (EBS2, EBS3, EBS5) (Fig. 3), 3 different sporulating strains of fungal isolates from leaves (EFL1, EFL2, EFL3) and 1 non-sporulating yeast species (EFS3) from the stem (Fig. 4) were selected and subjected to biochemical characterization and molecular identification. From biochemical analysis 75% of the bacterial isolate were Gram positive, 25% were Gram negative. Observations from macroscopic and biochemical characterisation of endophytic bacteria are summarised in Table 1.

The macroscopic and microscopic observations of the fungal isolates such as colony characteristics, colour of the colony, mycelium, spore formation, structure and morphology of conidiophores and conidia are shown in Table 2. The morphological characteristics of the yeast species is confirmed by the urease test and it is illustrated in Table 3.

3.2.2 Molecular identification and phylogenetic analysis

The 16S rRNA gene sequence of 8 bacterial endophytes and the 18S rDNA gene sequence of 3 fungal and 1yeast

Table 2 Phenotypic identification of fungal endophytes

S.No	Sample Marking	Macroscopic Observation	Microscopic Observation		
			Mycelium	Spores	Structure & Morphology
1	EFL1	Yellowish brown color colonies Brown color spores	Branched Hyphae	+	Conidiophores biverticillate Conidia are globose to subglobose
2	EFL2	Colonies are flat, powdery or velvety in texture Yellow-brown	Septate hyaline hyphae	+	conidiophores, phialides, conidia, and chlamydospores are observed
3	EFL3	White rough Mycelium, light green color Spores	Branched With Septate Hyphae	+	Conidiophore, Chain Conidiophores are observed

Table 3 Phenotypic identification of Yeast Endophytes

S.No	Sample Marking	Macroscopic Observation	Microscopic Observation Mycelium	Urease test
1	EFL1	Creamy white Round Colonies	Gram Positive Cocci like Structure	Urease positive, appearance of pink color

Table 4 BLAST results of the sequence analyzed from endophytes

S.No	Colony Code	Sequence analysis	Possible genus	Related strains (from GenBank sequences)	Genebank accession number	Query cover (%)	Identity (%)
1	EBL1	16S rRNA	*Micrococcus luteus*	*Micrococcus luteus* strain NCTC 2665	NR_075062.2	100	99.66
				Micrococcus yunnanensis strain YIM	NR_116578.1	95	99.79
				Micrococcus antarcticus strain T2	NR_025285.1	100	98.38
2	EBL3	16S rRNA	*Chryseomicro-bium palamuruense*	*Chryseomicrobium palamuruense* strain PU1	NR_151985.1	98	97.94
				Chryseomicrobium amylolyticum strain JC16	NR_108459.1	96	98.11
				Chryseomicrobium aureum strain BUT-2	NR_134003.1	96	97.63
3	EBL4	16S rRNA	*Cupriavidus metallidurans*	*Cupriavidus metallidurans* strain CH34	NR_074704.1	100	98.99
				Cupriavidus necator strain N-1	NR_102851.1	100	98.53
				Cupriavidus plantarum strain ASC-64	NR_109160.1	99	98.78
4	EBL6	16S rRNA	*Bacillus kochii*	*Bacillus kochii* strain WCC 4582	NR_117050.1	98	99.67
				Bacillus gottheilii strain WCC 4585	NR_108491.1	98	97.20
				Bacillus ciccensis strain 5L6	NR_159148.1	97	97.00
5	EBL9	16S rRNA	*Staphylococcus saprophyticus*	*Staphylococcus saprophyticus* subsp. saprophyticus strain ATCC 15305	NR_074999.2	100	99.14
				Staphylococcus gallinarum strain VIII1 16S ribosomal RNA gene	NR_036903.1	97	99.86
				Staphylococcus edaphicus strain CCM 8730	NR_156818.1	100	99.07
6	EBS2	16S rRNA	*Bacillus australimaris*	*Bacillus australimaris* strain MCCC 1A05787	NR_148787.1	98	99.87
				Bacillus stratosphericus strain 41KF2a	NR_042336.1	99	99.54
				Bacillus zhangzhouensis strain MCCC 1A08372	NR_148786.1	98	99.80
7	EBS3	16S rRNA	*Bacillus subtilis*	*Bacillus subtilis* strain DSM 10	NR_027552.1	99	100
				Bacillus subtilis strain IAM 12118	NR_112116.2	99	99.93
				Bacillus subtilis subsp. inaquosorum strain BGSC 3A28	NR_104873.1	99	99.93
8	EBS5	16S rRNA	*Pantoea anthophila*	*Pantoea anthophila* strain LMG 2558	NR_116113.1	99	99.58
				Pantoea allii strain BD 390	NR_115258.1	99	99.02
				Pantoea deleyi strain LMG 24200	NR_116114.1	99	99.09
9	EFL1	18S rDNA	*Talaromyces marneffei*	*Talaromyces marneffei* strain TM4 chromosome 3	CP015870.1	100	95.53
				Talaromyces pinophilus strain 1-95	CP017345.1	100	95.54
				Penicillium verruculosum	AF510496.1	100	95.42
10	EFL2	18S rDNA	*Paecilomyces variotii*	*Paecilomyces variotii* strain ATCC 10865	FJ345354.1	100	98.86
				*Byssochlamys spectabilis*isolate SAN1126	KC311513.1	85	99.40
				Paecilomyces tabacinus	LT548280.1	88	95.55

Table 4 Continued

S.No	Colony Code	Sequence analysis	Possible genus	Related strains (from GenBank sequences)	Genebank accession number	Query cover (%)	Identity (%)
11	EFL3	18S rDNA	*Penicillium verruculosum*	*Penicillium verruculosum*	AF510496.1	100	98.32
				Talaromyces pinophilus	CP017345.1	100	98.26
				Talaromyces marneffei	CP015870.1	100	98.03
12	EFS1	18S rDNA	*Cryptococcus neoformans*	*Cryptococcus* sp. P40A001	JX188145.1	84	97.08
				Bullera unica strain CB12	KM232490.1	92	91.15
				Cryptococcus flavescens	FN428902.1	65	99.91

Table 5 GenBank accession data of endophytes from *W. indica*

S.No	Colony	Homologous Microorganisms (% identity)	Genbank iD
1	EBL1	*Micrococcus luteus* (99.6)	MN075406
2	EBL3	*Chryseomicrobium palamuruense* (97.94)	MN075509
3	EBL4	*Cupriavidus metallidurans* (98.99)	MN075512
4	EBL6	*Bacillus kochii* (99.67)	MN075515
5	EBL9	*Staphylococcus saprophyticus* (99.14)	MN077137
6	EBS2	*Bacillus australimaris* (99.87)	MN077148
7	EBS3	*Bacillus subtilis* (100)	MN07714
8	EBS5	*Pantoea anthophila* (99.58)	MN077163
9	EFL1	*Talaromyces marneffei* (95.53)	MN077570
10	EFL2	*Paecilomyces variotii* (98.86)	MN077514
11	EFL3	*Penicillium verruculosum* (98.32)	MN077562
12	EFS1	*Cryptococcus neoformans* (97.08)	MN077561

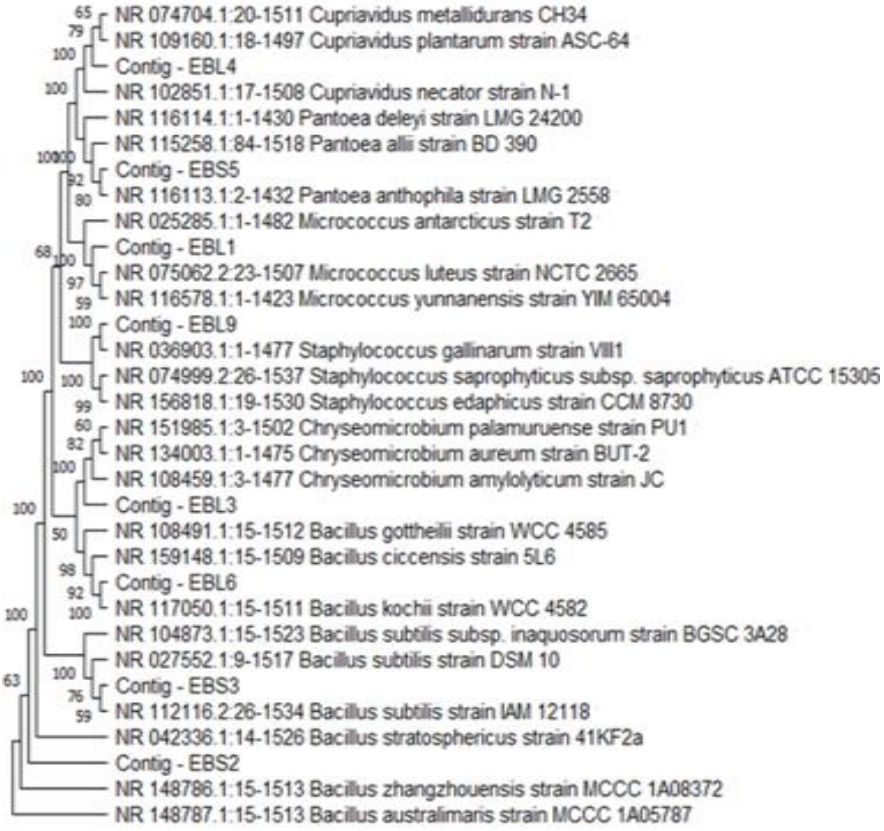

Fig. 5 Phenogram of bacterial endophytes

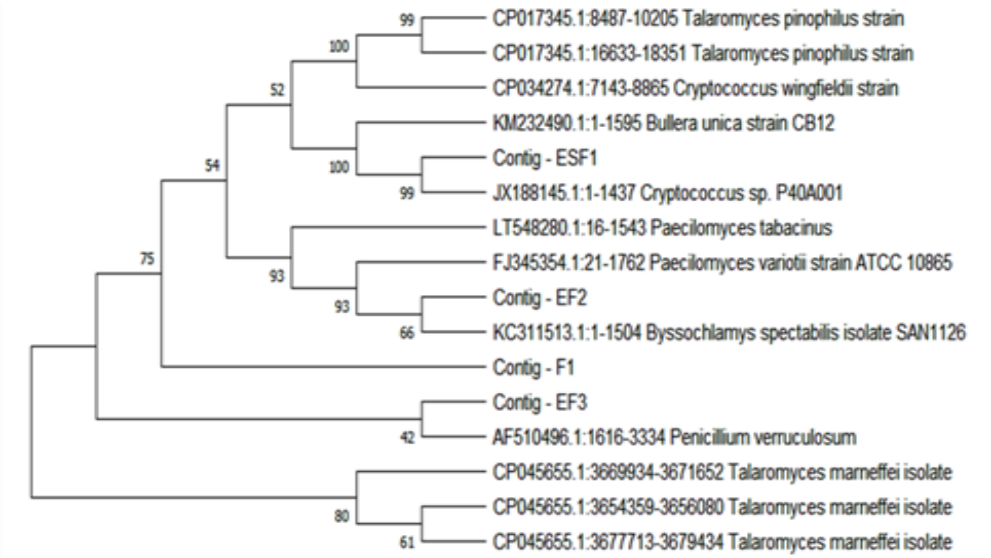

Fig. 6 Phenogram of fungal and yeast endophytes

isolates were used to barcode the genera and species through sequencing analysis and advanced BLAST search program at NCBI (Altschul *et al.* 1990). The query sequence length of bacteria is approximately 1500 bp and that of fungi was between 1698 to 1756 bp. The first three closely related hits of each isolates from GenBank with its accession number, identity and query cover are shown in Table 4. The nucleotide sequence data of the endophytes was then deposited to the GenBank and accession number was obtained (Table 5). Each isolates showed 97-99% of high similarity with the corresponding strains.

The phylogenetic analysis performed using MEGA X involved 32 nucleotide sequences in 1553 positions in the final data set of bacteria and 16 nucleotide sequences in 2210 positions for fungi. Phonetic and genetic study confirmed that the isolates were closely related to the different type of strains. The phenogram of each isolates to their taxonomically similar groups is depicted in Fig. 5 and Fig. 6 respectively.

The enumerated endophytic bacteria such as *Micrococcus luteus*, *Bacillus* sp., (*Bacillus australimaris*, *Bacillus subtilis*, *Bacillus kochii*), *Pantoea anthophila*, and *Staphylococcus saprophyticus* are commonly found in internal tissues of many agronomic plants like maize, rice, wheat, red clover, apple, papaya fruit, strawberry, grapevine etc., (Afzal *et al.* 2019). They stimulate plant growth by producing growth hormones, help in plant adaptation in drought conditions, induce host defence gene expression, and aids in biodegradation (Arora *et al.* 2010, Gond *et al.* 2015, Kavamura *et al*. 2013, Neetha *et al*. 2018). *Cupriavidus metallidurans* is a metal resistant soil bacterium, also isolated from sludge, legume nodules (Andam *et al.* 2007) and contributes to the phytoextraction of toxic metals (Vicentin *et al*. 2018). The bacteria increased plant growth significantly and involved in nodule nitrogenase activity (Barrett and Parker 2006). For the first time, the organism's localization in leaves was identified in our study. *Chryseomicrobium* sp., belongs to Planococcaceae family hitherto isolated from semi-arid tropical soil (Raj *et al*. 2013) sediment sample of a drainage (Pindi *et al*. 2016), seawater (Arora *et al*. 2010), and activated sludge (Deng *et al*. 2014). This is the first report for the species as an endophyte that has 98% sequence similarity with *Chryseomicrobium palamuruense*.

Endophytic fungi such as *Talaromyces* sp, *Paecilomyces* sp, and *Penicillium* sp isolated from different medicinal plants have also been identified in leaves of *W. indica*. They are a potential source of biologically active metabolites, phytohormones that influence plant growth and health, enhances antagonistic property, and helps to adapt host plant to stress conditions (Amatuzzi *et al*. 2018, Bilal *et al*. 2017, Sahu *et al*. 2019).

An endophytic yeast *Cryptococcus flavescens* was identified in the stem of *W. indica*. Similar *Cryptococcus* genus was reported earlier in sweet orange and cactus that may be a source of bioactive molecules to inhibit or control plant disease pathogens (Gai *et al*. 2009, Silva-Hughes *et al*. 2015). This study on isolation and identification of endophytic microorganisms from the leaf and stem parts of *W. indica* is the first report from the Kanjamalai foothills of Salem district, Tamilnadu.

3.3 Biosynthesis of silver nanoparticles

The heavy metal resistant property of *Cupriavidus metallidurans* may support biologically stable NPs production. The formation of NPs from the bacterial aqueous filtrate (Yellow colour) incubated with $AgNO_3$ solution was scrutinized after 24 hours visually by the color change to dark brown (Fig. 7). No color change was observed in the control. The colour change may be due to the reduction of silver ions to nano silver by the bioactive compounds in the extracellular endophytic extract. This reduction process may lead to the excitation of surface plasmon resonance (SPR) in AgNPs that can be measured by spectroscopic methods. About 1L of bacterial AgNPs solution contained 100 mg of *Cm*-AgNPs pellets.

Fig. 7 Biosynthesis of silver nanoparticles

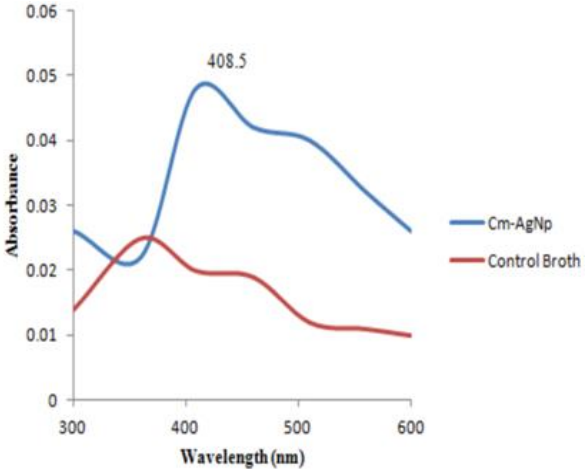

Fig. 8 UV-visible spectrum of *Cm*-AgNPs

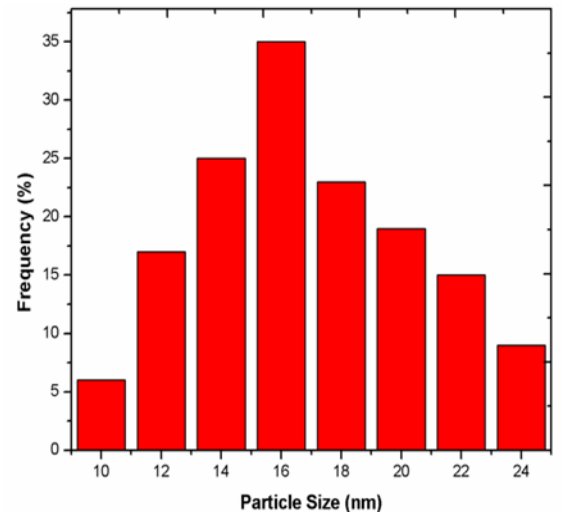

Fig. 9 DLS analysis of *Cm*-AgNPs

3.4 Characterization studies of silver nanoparticles

AgNPs corresponds to the SPR peak between 400–450 nm in the UV-visible spectra (Mie *et al*. 2014). This phenomenon is due to the oscillation of free electrons in Ag with reflected light, size, shape of AgNPs and their association with bacterial metabolites. The reaction mixture of *Cm*-AgNPs exhibited a smooth absorbance peak at the wavelength 408.5nm that confirms the presence of AgNPs.

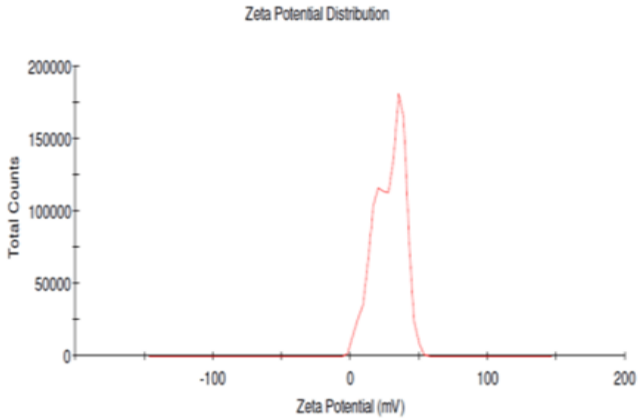

Fig. 10 Zeta potential of the *Cm*-AgNPs

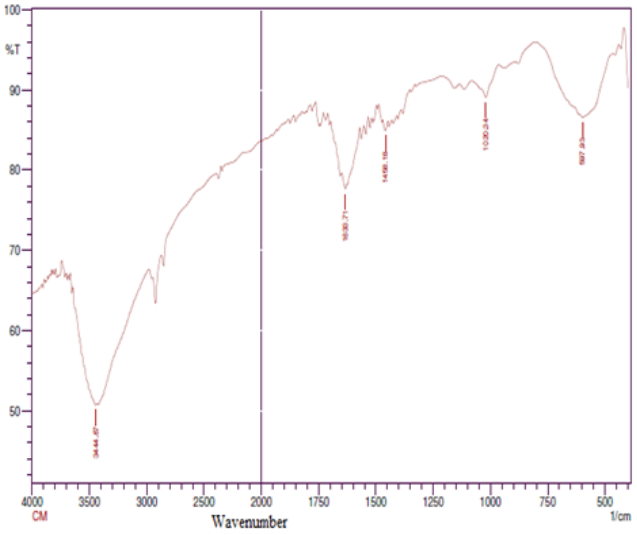

Fig. 11 FTIR spectrum of *Cm*-AgNPs

Similar results were reported in many studies related to the biosynthesis of AgNPs (Anandalakshmi *et al*. 2016, Wang *et al*. 2020) (Fig. 8) that exhibited good antimicrobial activity.

The size and surface charge influence the effectiveness of the AgNPs. The DLS analysis (Fig. 9) shows that the average size of *Cm*-AgNPs was 16 nm and the size varied from 10-24 nm. The zeta potential of the *Cm*-AgNPs was found as a sharp peak at 28.2 mV which indicates that the surface of synthesized NPs was positively charged (Fig. 10). The endophytic metabolites capping the surface of NP may attribute to the positive charge. The zeta spectrum also shows that the NPs is stable and have strong precipitation and agglomeration (Riddick 1968). The values obtained were comparable to the zeta potential of biosynthesized NPs reported by Ali *et al*. 2016, Selvarani 2015).

FTIR spectrum revealed the presence of different bands at 3444.87, 1633.71, 1458.18, 1020.34, 597.93cm−1 (Fig. 11). The peak at 3444.87cm^{-1} corresponds to the O-H stretching vibrations of water molecules. The bands at 1633.71cm^{-1} and 1458.18cm^{-1} shows C=C Stretching vibrations of non-conjugated, disubstituted alkene group and C-H bending vibrations of CH_3 group respectively. The band at 1020.34 cm−1 can be assigned to medium C–N

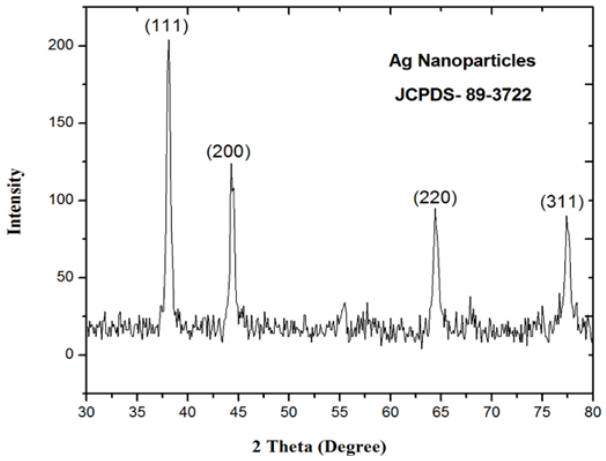

Fig. 12 XRD pattern of *Cm*-AgNPs

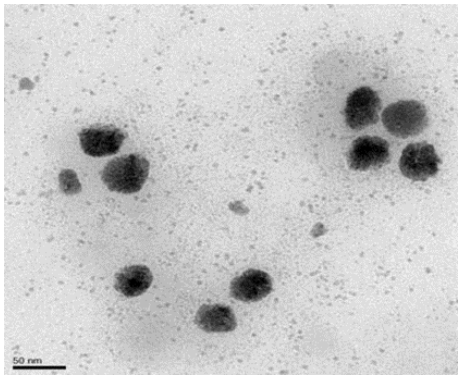

Fig. 13 TEM Image of *Cm*-AgNPs

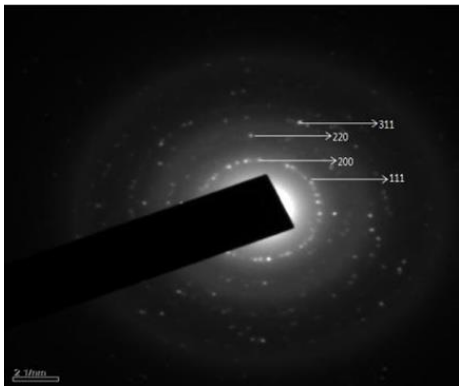

Fig. 14 SAED pattern of *Cm*-AgNPs

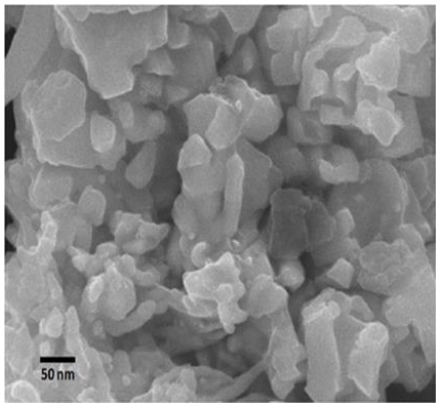

Fig. 15 SEM image of *Cm*-AgNPs

stretching vibrations of amines signifying the presence of amino acid. The peak obtained at 597.93cm^{-1} region could be attributed to alkyl halides stretching. The observation confirms the presence of hydroxyl, alkene and amine groups in the bacterial extract that act as reducing capping and stabilizing agents of AgNPs as reported in early findings (Roseline *et al*. 2019, Singh *et al*. 2014).

XRD analysis showed the strongest diffraction peaks at 2θ values of 38.12°, 44.31°, 64.46° and 77.41° (Fig. 12). These peaks are assigned to 111, 200, 220 and 311 planes of a face centre cubic structure of *Cm*-AgNPs that agrees with the JCPDS file no. 89-3722 for silver. By using the Debye-Scherrer equation, the average size of crystallite *Cm*-AgNPs was found to be 16.4 nm. No secondary peaks were observed in the XRD pattern thus confirms the pure crystalline nature of AgNP as mentioned in the previous reports of green synthesized NPs from endophytic bacteria, fungi and plant extracts (Dong *et al*. 2017, Gnanadesigan *et al*. 2011, Singh *et al*. 2017). The size obtained in the XRD pattern excellently confirms the average size obtained in DLS analysis.

TEM micrograph (Fig. 13) showed an average size of 18±0.5nm for *Cm*-AgNPs. Circular aggregates with smooth edges were observed that are not in direct contact with each other. It shows that the AgNPs are stabilized by capping agents from the endophytic extract. Fig. 14 shows the SAED pattern of *Cm*-AgNPs in 111, 200, 220, 311 planes matching with diffraction rings that were in agreement with XRD data. The presence of bright spots within the diffraction rings of crystal orientations confirms the FCC structure with polycrystalline nature of AgNPs. The average size of the particle was also nearly in equivalence with DLS analysis. The results obtained were comparable to former reports of green synthesized AgNPs by Devi and Joshi. (2015), Devaraj *et al*. (2013). The small size of NPs may enhance the reactivity and catalytic activity in various applications.

SEM image depicted additional data on the shape and dimension of the *Cm*-AgNPs synthesized from endophytic extract (Fig. 15). It showed that the *Cm*-AgNPs is irregularly shaped, nonuniform polydispersed with an average size of 50 nm. The smaller particles may aggregate to give the large-size appearance of nanoparticles (Devaraj *et al*. 2013). The large particle size depicted in SEM compared to DLS and XRD may be due to the difference in sample preparation and the presence of various forces of interaction in the solution (Banerjee and Nath 2015).

The EDX profile (Fig. 16) showed a sharp absorption peak between 3–4keV, that is typical to metallic AgNPs. No additional peak was observed. Thus *Cm*-AgNPs was biosynthesized successfully from endophytic bacterial extracts that was similar to the earlier reports of Ghosh *et al*. (2012) and Singh *et al*. (2017). The weight of silver was found to be 43.69 % thus confirms *Cm*-AgNPs was successfully biosynthesized from endophytic bacterial extracts.

3.5 Antimicrobial activity of silver nanoparticles

The antimicrobial activity of the *Cm*-AgNPs was checked by agar well diffusion method against Gram-

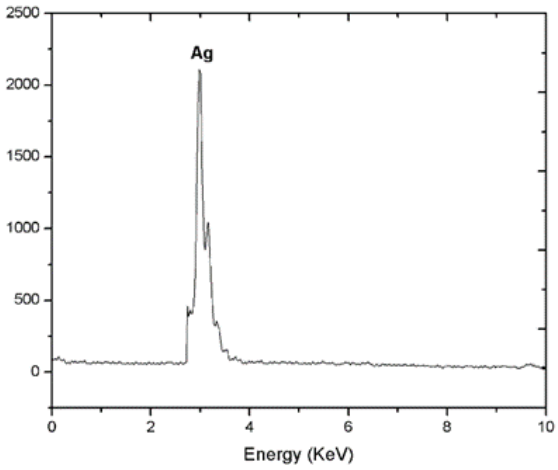

Fig. 16 EDX profile of *Cm*-AgNPs

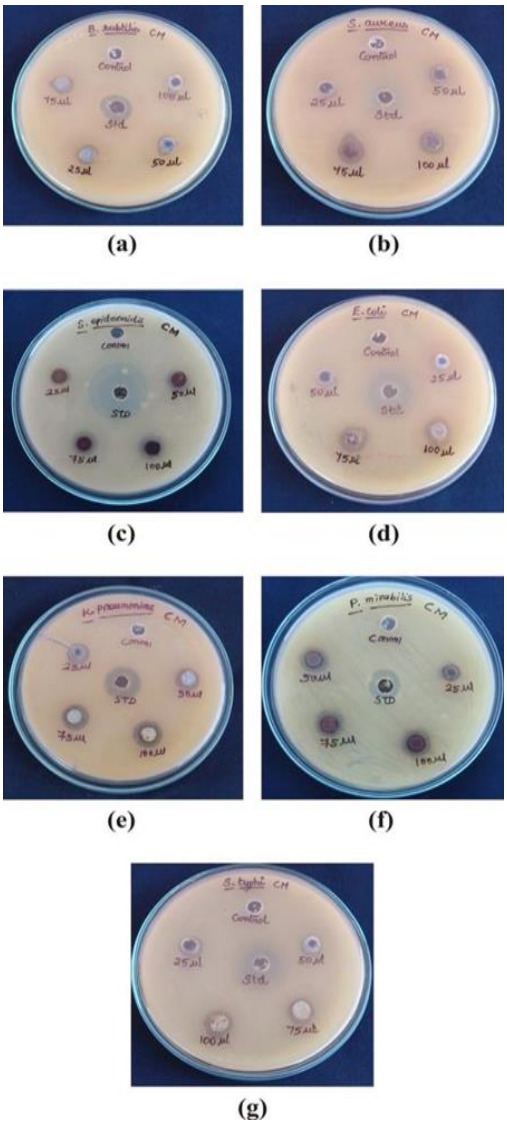

Fig. 17 Antibacterial activity of *Cm*-AgNPs

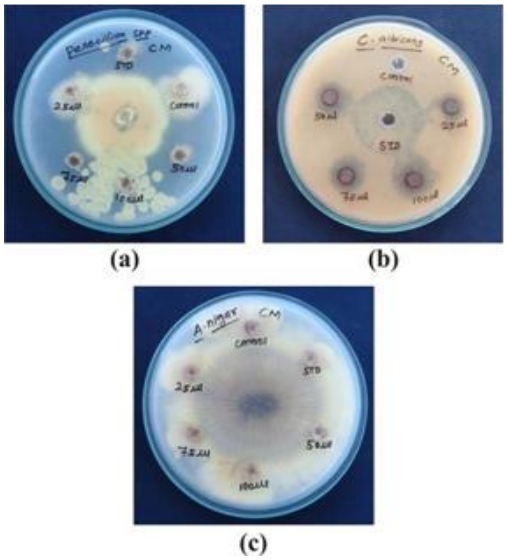

Fig. 18 Antifungal activity of *Cm*-AgNPs

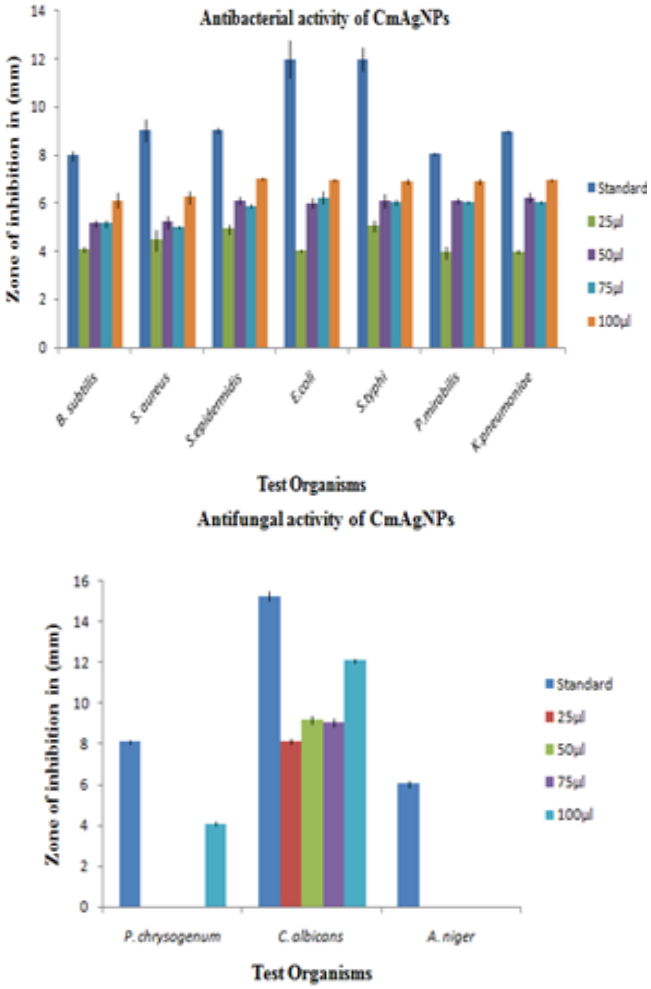

Fig. 19 Zone of inhibition for pathogens

positive, Gram-negative human pathogenic bacteria and fungal pathogens. *Cm*-AgNPs showed remarkable anti-bacterial activity with maximum inhibition of 7.03±0.06 mm and a minimum inhibition of 3.97±0.25 mm. There was significant antibacterial action against *S.epidermidis*, *E.coli*, *S.typhi*, *K.pneumonia*, and *P.mirabilis* and a moderate action against *B. subtilis*, and *S. aureus* (Fig. 17). Comparatively low activity was observed against *P. mirabilis* (3.97±0.25 mm) but at higher concentration the

Table 6 Antibacterial activity of *Cm*-AgNPs against selected bacterial strains

S.No	Test Organisms	ZOI of *Cm*-AgNPs					
		Standard (mm)	Control (mm)	25µl (mm)	50µl (mm)	75µl (mm)	100µl (mm)
1	*B. subtilis*	8±0.20	-	4.10±0.10	5.17±0.15	5.17±0.15	6.13±0.32
2	*S. aureus*	9.03±0.45	-	4.47±0.45	5.23±0.25	5.03±0.06	6.27±0.25
3	*S. epidermidis*	9.07±0.12	-	4.93±0.21	6.13±0.15	5.90±0.10	7.03±0.06
4	*E. coli*	12±0.80	-	4.03±0.06	6.0±0.20	6.23±0.25	6.97±0.06
5	*S. typhi*	12±0.50	-	5.07±0.21	6.10±0.26	6.07±0.12	6.93±0.12
6	*P. mirabilis*	8.03±0.06	-	3.97±0.25	6.10±0.10	6.03±0.06	6.93±0.12
7	*K. pneumoniae*	8.97±0.06	-	4±0.10	6.23±0.21	6.03±0.06	6.97±0.06

Table 7 Antifungal Activity of *Cm*-AgNPs against selected fungal strains

S.No	Test Organisms	ZOI of *Cm*-AgNPs					
		Standard (mm)	Control (mm)	25µl (mm)	50µl (mm)	75µl (mm)	100µl (mm)
1	*P. chrysogenum*	8.10±0.10	-	-	-	-	4.10±0.10
2	*C. albicans*	15.27±0.25	-	8.13±0.15	9.20±0.20	9.07±0.21	12.10±0.10
3	*A. niger*	6.03±0.15	-	-	-	-	-

Table 8 Antimicrobial activity of NPs from *Cupriavidus* sp., from various sources

S.No	Microorganisms	NPs	Antimicrobial Property	Pathogenic Organisms	References
1	*C. metallidurans*	Gold nano-particles (AuNPs)	No activity	*E.coli* MG1655	Montero-Silva *et al*., 2018
2	*C. metallidurans*	AgNPs	Antibacterial activity	*E.coli* MG1655	Montero-Silva *et al*., 2018
3	*Cuprividus* sp., from soil	AgNPs	Antibacterial activity	*Stenotrophomonas pavanii*, *Aeromonas enteropelogenes*, *Proteus mirabilis*, *Enterobacter xiangfangensis*	Ameen *et al*., 2020
4	*C. metallidurans* from leaf of *W.indica*	AgNPs	Antibacterial activity	*B. subtilis*, *S. aureus*, *S. epidermidis*, *E. coli*, *S. typhi*, *P. mirabilis*, *K. pneumoniae*	Our study
5	*C. metallidurans* from leaf of *W.indica*	AgNPs	Antifungal activity	*P. chrysogenum*, *C. albicans*, *A. niger*	Our study

inhibition was 6.93±0.12 mm. Broad-spectrum activity of the *Cm*-AgNPs against the five pathogenic bacteria was significant. There was substantial antibacterial activity at the concentration of 25µg/mL and the activity increased with an increase in dose level of 100µg/mL. The diameters of the inhibition zones for the all tested pathogens are illustrated in Fig. 19 (Table 6, Table 7). There was no inhibition zone observed for *A.niger*, while *Penicillium chrysogenum* was inhibited only at a higher concentration of 100µg/mL (4.10±0.10). *Candida albicans* was inhibited maximally (Fig. 18) than bacterial pathogens with inhibition zone between 8.13±0.15 mm to 12.10±0.10 mm. The results were compared with standard drugs used as positive controls. Negative control plates didn't express any inhibition zones. Similar results were obtained in recent studies of Monowar *et al*. (2018), Sunkar and Nachiyar (2012) who reported the promising antimicrobial activity of AgNPs from endophytes.

AgNPs are remarkably known for their antimicrobial activity, yet the judicious mechanism attributing the property is ambiguous. AgNPs damage the membrane lipids and deteriorates membrane function (Qian *et al*. 2013), denature the proteins, induce oxidative stress and finally direct to cell death. The prevalence of multidrug resistant direct to cell death. The prevalence of multidrug resistant bacteria and pandemic viruses led to the development of AgNPs based drug candidates with high resistance property. *Cm*-AgNPs showed broad spectrum activity against the pathogenic organisms used. This may be due to the higher concentration of AgNPs that breaks the peptidoglycan layers of Gram-positive and Gram-negative bacteria than at the lower concentrations. The average smaller size of 16.4nm and the positive surface charge of *Cm*-AgNPs also attributes to the bactericidal property that was in concurrence with the earlier reports (Levard *et al*. 2012, Nirmala and Sridevi 2021). Table 8 compares the antimicrobial activity of NPs from *Cupriavidus* sp., from various sources. The promising results obtained against various microbes may help in developing biosynthesised NPs as potent antimicrobial agents.

4. Conclusions

The present study provides the first report on the exploration of endophytic population associated with the

stem and leaves of *W. indica*, a medicinal plant widely used in many pharmacological formulations. This study provides evidence for the presence of some novel groups that can be exploited for producing bioactive moieties for various medical applications. An ecofriendly and cost-effective method for AgNPs synthesis was carried out using an endophytic bacterium *Cupriavidus metallidurans* isolated from the leaf of the plant. The structural characterization of *Cm*-AgNPs showed absorption peak 408.5nm with an average size of 16.4 nm with positive surface potential. The XRD, FTIR, SEM, and EDX revealed the optimal formation with crystalline nature and elemental composition of Ag. *Cm*-AgNPs exhibited potential antimicrobial activity against 10 different pathogens. Thus a cost-effective, substantial eco-friendly method of AgNPs was proposed that may shift the nanoscience research to the endophytic avenue for effective green synthesis methodology. With this prior art, the activity of endophytic AgNPs can be explored further as an optimistic therapeutic in the treatment of cancer, inflammations etc.

Acknowledgments

The authors gratefully acknowledge Department of Biotechnology, Vinayaka Mission's Kirupananda Variyar Engineering College, Salem and Acme ProGen Biotech (India) Private Limited, Salem for providing the essential facilities to carry out the research.

References

Abrahamson, J.T., Sempere, B., Walsh, M.P., Forman, J.M., Sen, F., Sen, S., Mahajan, S.G., Paulus, G.L., Wang, Q.H., Choi, W. and Strano, M.S. (2013), "Excess thermopower and the theory of thermopower waves", *Acs Nano*, **7**(8), 6533-6544. https://doi.org/10.1021/nn402411k.

Afzal, I., Shinwari, Z.K., Sikandar, S. and Shahzad, S. (2019), "Plant beneficial endophytic bacteria: Mechanisms, diversity, host range and genetic determinants", *Microbiol. Res.*, **221**, 36-49. https://doi.org/10.1016/j.micres.2019.02.001.

Ali, Z. A., Yahya, R., Sekaran, S. D. and Puteh, R. (2016), "Green synthesis of silver nanoparticles using apple extract and its antibacterial properties", *Adv. Mater. Sci. Eng.*, 410219. https://doi.org/10.1155/2016/4102196.

Altschul, S.F., Gish, W., Miller, W., Myers, E.W. and Lipman, D.J. (1990), "Basic local alignment search tool", *J. Mol. Biol.*, **215**(3), 403-10. https://doi.org/10.1016/S0022-2836(05)80360-2.

Amatuzzi, R.F., Cardoso, N., Poltronieri, A.S., Poitevin, C.G., Dalzoto, P., Zawadeneak, M.A., Pimentel, I.C. (2018), "Potential of endophytic fungi as biocontrol agents of *Duponchelia fovealis* (Zeller) (Lepidoptera: Crambidae)", *Brazil. J. Biol.*, **78**(3), 429-35. https://doi.org/10.1590/1519-6984.166681.

Ameen, F., AlYahya, S., Govarthanan, M., ALjahdali, N., Al-Enazi, N., Alsamhary, K., Alshehri, W.A., Alwakeel, S.S. and Alharbi, S.A. (2020), "Soil bacteria *Cupriavidus* sp. mediates the extracellular synthesis of antibacterial silver nanoparticles", *J. Mol. Struct.*, **1202**, 127233. https://doi.org/10.1016/j.molstruc.2019.127233.

Anandalakshmi, K., Venugobal, J. and Ramasamy, V. (2016), "Characterization of silver nanoparticles by green synthesis method using *Pedalium murex* leaf extract and their antibacterial activity", *Appl. Nanosci.*, **6**(3), 399-408. https://doi.org/10.1007/s13204-015-0449-z.

Andam, C.P., Mondo, S.J. and Parker, M.A. (2007), "Monophyly of nodA and nifH genes across Texan and Costa Rican populations of Cupriavidus nodule symbionts", *Appl. Environ. Microbiol.*, **73**(14), 4686-90. https://doi.org/10.1128/AEM.00160-07.

Arora, N.K., Khare, E. and Maheshwari, D.K. (2010), "Plant growth promoting rhizobacteria: Constraints in bioformulation, commercialization, and future strategies", *InPlant Growth Health Promot. Bacteria*, 97-116. https://doi.org/10.1007/978-3-642-13612-2_5.

Banerjee, P. and Nath, D. (2015), "A phytochemical approach to synthesize silver nanoparticles for non-toxic biomedical application and study on their antibacterial efficacy", *Nanosci. Technol*, **2**(1), 1-4.

Barnett, H.L. and Hunter, B.B. (1998), *Illustrated genera of imperfect fungi*, APS Press.

Barrett, C.F. and Parker, M.A. (2006), "Coexistence of *Burkholderia*, *Cupriavidus*, and *Rhizobium* sp. nodule bacteria on two *Mimosa* spp. in Costa Rica", *Appl. Environ. Microbiol.*, **72**(2), 1198-206. https://doi.org/10.1128/AEM.72.2.1198-1206.2006.

Bilal, S., Khan, A.L., Shahzad, R., Asaf, S., Kang, S.M. and Lee, I.J. (2017), "Endophytic *Paecilomyces formosus* LHL10 augments Glycine max L. adaptation to Ni-contamination through affecting endogenous phytohormones and oxidative stress", *Front. Plant Sci.*, **8**, 870. https://doi.org/10.3389/fpls.2017.00870.

Buchanan, R.E. and Gibbons, N.E. (1975), *Bergey's Manual of Determinative Bacteriology*, Williams & Wilkins.

Chockalingam, N. and Muruhan, S. (2017), "Anti-inflammatory properties of rosmarinic acid- a review", *Int. J. Res. Pharmaceut. Sci.*, **8**(4), 656-62.

Correll, J.C., Klittich, C.J. and Leslie, J.F. (1987), "Nitrate nonutilizing mutants of *Fusarium oxysporum* and their use in vegetative compatibility tests", *Phytopathology*, **77**(12), 1640-6.

Cullity, B.D. (1978), *Elements of X-ray diffraction*, *Addison-Wesley*.

Deepak, P., Amutha, V., Kamaraj, C., Balasubramani, G., Aiswarya, D. and Perumal, P. (2019), *Chemical and green synthesis of nanoparticles and their efficacy on cancer cells*, In *Green Synthesis, Characterization and Applications of Nanoparticles*, 369-387, Elsevier. https://doi.org/10.1016/B978-0-08-102579-6.00016-2.

Deng, S.K., Ye, X.M., Chu, C.W., Jiang, J., He, J., Zhang, J. and Li, S.P. (2014), "*Chryseomicrobium aureum* sp. nov., a bacterium isolated from activated sludge", *Int. J. Syst. Evol. Microbiol.*, **64**(8), 2682-2687. https://doi.org/10.1099/ijs.0.061143-0.

Devaraj, P., Kumari, P., Aarti, C. and Renganathan, A. (2013), "Synthesis and characterization of silver nanoparticles using cannonball leaves and their cytotoxic activity against MCF-7 cell line", *J. Nanotechnol.*, 598328. https://doi.org/10.1155/2013/598328.

Devi, L.S. and Joshi, S.R. (2015), "Ultrastructures of silver nanoparticles biosynthesized using endophytic fungi", *J. Microscop. Ultrastruct.*, ***3***(1), 29-37. https://doi.org/10.1016/j.jmau.2014.10.004.

Diantoro, M., Suprayogi, T., Sa'adah, U., Mufti, N., Fuad, A., Hidayat, A. and Nur, H. (2018), *Modification of Electrical Properties of Silver Nanoparticle*, in *Silver Nanoparticles: Fabrication, Characterization and Applications*, 233. https://doi.org/10.5772/intechopen.75682.

Dong, Z.Y., Narsing Rao, M.P., Xiao, M., Wang, H.F., Hozzein, W.N., Chen, W. and Li, W.J. (2017), "Antibacterial activity of silver nanoparticles against *Staphylococcus warneri* synthesized using endophytic bacteria by photo-irradiation", *Front.*

Microbiol., **8**, 1090. https://doi.org/10.3389/fmicb.2017.01090.
Felsenstein, J. (1985), "Confidence limits on phylogenies: an approach using the bootstrap", *Evolution*, **39**(4), 783-791. https://doi.org/10.1111/j.1558-5646.1985.tb00420.x.
Frank, J.A., Reich, C.I., Sharma, S., Weisbaum, J.S., Wilson, B.A. and Olsen, G.J. (2008), "Critical evaluation of two primers commonly used for amplification of bacterial 16S rRNA genes", *Appl. Environ. Microbiol*., **74**(8), 2461-2470. https://doi.org/10.1128/AEM.02272-07.
Gai, C.S., Lacava, P.T., Maccheroni Jr, W., Glienke, C., Araújo, W.L., Miller, T.A. and Azevedo, J.L. (2009), "Diversity of endophytic yeasts from sweet orange and their localization by scanning electron microscopy", *J. Basic Microbiol*., **49**(5), 441-451. https://doi.org/10.1002/jobm.200800328.
Ghosh, S., Patil, S., Ahire, M., Kitture, R., Kale, S., Pardesi, K., Cameotra, S.S., Bellare, J., Dhavale, D.D., Jabgunde, A. and Chopade, B.A. (2012), "Synthesis of silver nanoparticles using *Dioscorea bulbifera* tuber extract and evaluation of its synergistic potential in combination with antimicrobial agents", *Int. J. Nanomed*., **7**, 483. https://doi.org/10.2147/IJN.S24793.
Gnanadesigan, M., Anand, M., Ravikumar, S., Maruthupandy, M., Vijayakumar, V., Selvam, S., Dhineshkumar, M. and Kumaraguru, A.K. (2011), "Biosynthesis of silver nanoparticles by using mangrove plant extract and their potential mosquito larvicidal property", *Asia. Pac. J. Tropical Med*., **4**(10), 799-803. https://doi.org/10.1016/S1995-7645(11)60197-1.
Göksu, H., Çelik, B., Yıldız, Y., Şen, F. and Kılbaş, B. (2016), "Superior monodisperse CNT-supported CoPd (CoPd@ CNT) nanoparticles for selective reduction of nitro compounds to primary amines with $NaBH_4$ in aqueous medium", *Chem. Select*, **1**(10), 2366-2372. https://doi.org/10.1002/slct.201600509.
Goksu, H., Sert, H., Kilbas, B. and Sen, F. (2017), "Recent advances in the reduction of nitro compounds by heterogenous catalysts", *Curr. Org. Chem*., **21**(9), 794-820.
Gond, S.K., Bergen, M.S., Torres, M.S., White Jr, J.F. (2015), "Endophytic Bacillus spp. produce antifungal lipopeptides and induce host defence gene expression in maize", *Microbiol. Res*., **172**, 79-87. https://doi.org/10.1016/j.micres.2014.11.004.
Iqbal, P., Preece, J.A. and Mendes, P.M. (2012), *Nanotechnology: The "Top-Down" and "Bottom-Up" Approaches*, in *Supramolecular Chemistry: From Molecules to Nanomaterials*, John Wiley & Sons, Ltd. https://doi.org/10.1002/9780470661345.smc195.
Kannan, M., Kumar, T.S. and Rao, M.V. (2016), "Antidiabetic and antioxidant properties of *Waltheria indica* L., an ethnomedicinal plant", *Int. J. Pharma. Res. Health Sci*, **4**(5), 1376-84. https://doi.org/10.21276/ijprhs.2016.05.07.
Kavamura, V.N., Santos, S.N., da Silva, J.L., Parma, M.M., Ávila, L.A., Visconti, A., Zucchi, T.D., Taketani, R.G. andreote, F.D., de Melo, I.S. (2013), "Screening of Brazilian cacti rhizobacteria for plant growth promotion under drought", *Microbiol. Res*., **168**(4), 183-91. https://doi.org/10.1016/j.micres.2012.12.002.
Kumar, S., Stecher, G., Li, M., Knyaz, C. and Tamura, K. (2018), "MEGA X: molecular evolutionary genetics analysis across computing platforms", *Mol. Biol. Evol*., **35**(6), 1547-1549. https://doi.org/10.1093/molbev/msy096.
Levard, C., Hotze, E.M., Lowry, G.V. and Brown Jr, G.E. (2012), "Environmental transformations of silver nanoparticles: impact on stability and toxicity", *Environ. Sci. Technol*., **46**(13), 6900-6914. https://doi.org/10.1021/es2037405.
Mariadoss, A.V.A., Ramachandran, V., Shalini, V., Agilan, B., Franklin, J.H., Sanjay, K., Alaa, Y.G., Tawfiq, M.A.A. and Ernest, D. (2019), "Green synthesis, characterization and antibacterial activity of silver nanoparticles by Malus domestica and its cytotoxic effect on (MCF-7) cell line", *Microbial Pathogenesis*., **135**, 103609. https://doi.org/10.1016/j.micpath.2019.103609.
Martin, K.J. and Rygiewicz, P.T. (2005), "Fungal-specific PCR primers developed for analysis of the ITS region of environmental DNA extracts", *BMC Microbiol*., **5**(1), 1-1. https://doi.org/10.1186/1471-2180-5-28.
Mie, R., Samsudin, M.W., Din, L.B., Ahmad, A., Ibrahim, N. and Adnan, S.N.A. (2014), "Synthesis of silver nanoparticles with antibacterial activity using the lichen *Parmotrema praesorediosum*", *Int. J. Nanomed*., **9**, 121. https://doi.org/10.2147/IJN.S52306.
Monowar, T., Rahman, M., Bhore, S.J., Raju, G. and Sathasivam, K.V. (2018), "Silver nanoparticles synthesized by using the endophytic bacterium *Pantoea ananatis* are promising antimicrobial agents against multidrug resistant bacteria", *Molecules*, **23**(12), 3220. https://doi.org/10.3390/molecules23123220.
Monteillier, A., Cretton, S., Ciclet, O., Marcourt, L., Ebrahimi, S.N., Christen, P. and Cuendet, M. (2017), "Cancer chemopreventive activity of compounds isolated from *Waltheria indica*", *J. Ethnopharmacol*., **203**, 214-25. https://doi.org/10.1016/j.jep.2017.03.048.
Montero-Silva, F., Durán, N. and Seeger, M. (2018), "Synthesis of extracellular gold nanoparticles using Cupriavidus metallidurans CH34 cells", *IET Nanobiotechnol*., ***12***(1), 40-46. https://doi.org/10.1049/iet-nbt.2017.0185.
Nair, D.N. and Padmavathy, S. (2014), "Impact of endophytic microorganisms on plants, environment and humans", *Sci. World J*., 250693. https://doi.org/10.1155/2014/250693.
Neetha, J.N., Ujwal, P., Sandesh, K., Santhosh, H. and Girish, K. (2018), "Aerobic biodegradation of Acid Blue-9 dye by *Bacillus fermus* Isolated from *Annona reticulate*", *Environ. Technol. Innov*., **11**, 253-261. https://doi.org/10.1016/j.eti.2018.06.007.
Nirmala, C. and Sridevi, M. (2021), "Characterization, antimicrobial and antioxidant evaluation of biofabricated silver nanoparticles from Endophytic *Pantoea anthophila*", *J. Inorg. Organomet. Polym. Mater*., **31**(9), 3711-3725. https://doi.org/10.1007/s10904-021-01974-7.
Nirmala, C., Sridevi, M. (2021), "Ethnobotanical, phytochemistry, and pharmacological property of *Waltheria Indica* Linn", *Future J. Pharm. Sci*., **7**, 14. https://doi.org/10.1186/s43094-020-00174-3.
Pindi, P.K., Ashwitha, K. and Rani, A.S. (2016), "*Chryseomicrobium palamuruense* sp. nov., a haloalkalitolerant bacterium isolated from a sediment sample", *Int. J. Syst. Evol. Microbiol*., **66**(9), 3731-3736. https://doi.org/10.1099/ijsem.0.001256.
Qian, Y., Yu, H., He, D., Yang, H., Wang, W., Wan, X. and Wang, L. (2013), "Biosynthesis of silver nanoparticles by the endophytic fungus *Epicoccum nigrum* and their activity against pathogenic fungi", *Bioproc. Biosyst. Eng*., **36**(11), 1613-1619. https://doi.org/10.1007/s00449-013-0937-z.
Qin, S., Li, J., Chen, H.H., Zhao, G.Z., Zhu, W.Y., Jiang, C.L., Xu, L.H. and Li, W.J. (2009), "Isolation, diversity, and antimicrobial activity of rare actinobacteria from medicinal plants of tropical rain forests in Xishuangbanna, China", *Appl. Environ. Microbiol*., **75**(19), 6176-6186. https://doi.org/10.1128/AEM.01034-09.
Rahman, S., Rahman, L., Khalil, A.T., Ali, N., Zia, D., Ali, M. and Shinwari, Z.K. (2019), "Endophyte-mediated synthesis of silver nanoparticles and their biological applications", *Appl. Microbiol. Biotechnol*., **103**(6), 2551-2569. https://doi.org/10.1007/s00253-019-09661-x.
Raj, P.S., Sasikala, C., Ramaprasad, E.V.V., Subhash, Y., Busse, H.J., Schumann, P. and Ramana, C.V. (2013), "*Chryseomicrobium amylolyticum* sp. nov., isolated from a semi-arid tropical soil, and emended descriptions of the genus Chryseomicrobium and *Chryseomicrobium imtechense*", *Int. J.*

Syst. Evol. Microbiol, **63**, 2612–2617. https://doi.org/10.1099/ijs.0.044552-0.

Riddick, T.M. (1968), "Control of colloid stability through zeta potential: Wth a closing chapter on its relationship to cardiovascular disease", *Zeta-Meter*, inc., 541.3453.

Roseline, T.A., Murugan, M., Sudhakar, M.P. and Arunkumar, K. (2019), "Nanopesticidal potential of silver nanocomposites synthesized from the aqueous extracts of red seaweeds", *Environ. Technol. Innov*., **13**, 82-93. https://doi.org/10.1016/j.eti.2018.10.005.

Sahu, S., Prakash, A. and Shende, K. (2019), *Talaromyces trachyspermus*, an endophyte from *Withania somnifera* with plant growth promoting attributes, *Environ. Sust*., **2**(1), 13-21. https://doi.org/10.1007/s42398-019-00045-5.

Saitou, N. and Nei, M. (1987), "The neighbor-joining method: a new method for reconstructing phylogenetic trees", *Mol. Biol. Evol*., **4**(4), 406-25. https://doi.org/10.1093/oxfordjournals.molbev.a040454.

Saravanakumar, K., Sriram, B., Sathiyaseelan, A., Hu, X., Mariadoss, A.V.A., MubarakAli, D. and Wang, M.H., (2021), "Molecular identification, volatile metabolites profiling, and bioactivities of an indigenous endophytic fungus (Diaporthe sp.)", *Proc. Biochem*., **102**, 72-81. https://doi.org/10.1016/j.procbio.2020.12.002.

Selvarani, S. (2015), "Anti-cancer activity of silver nanoparticle synthesized from stem extract of *Ocimum Kilimandscharicum* Against Hep-G2, liver cancer cell line", *J. Nanotech. Nanosci*., **1**, 100103.

Sen, B., Şavk, A. and Sen, F. (2018), "Highly efficient monodisperse Pt nanoparticles confined in the carbon black hybrid material for hydrogen liberation", *J. Colloid Interf. Sci*., **520**, 112-118. https://doi.org/10.1016/j.jcis.2018.03.004.

Silva-Hughes, A.F., Wedge, D.E., Cantrell, C.L., Carvalho, C.R., Pan, Z., Moraes, R.M., Madoxx, V.L. and Rosa, L.H. (2015), "Diversity and antifungal activity of the endophytic fungi associated with the native medicinal cactus *Opuntia humifusa* (Cactaceae) from the United States", *Microbiol. Res*., **175**, 67-77. https://doi.org/10.1002/jobm.200800328.

Singh, D., Rathod, V., Ninganagouda, S., Hiremath, J., Singh, A.K. and Mathew, J. (2014), "Optimization and characterization of silver nanoparticle by endophytic fungi *Penicillium* sp. isolated from *Curcuma longa* (turmeric) and application studies against MDR *E. coli* and *S. aureus*", *Bioinorg. Chem. Appl*., 408021. https://doi.org/10.1155/2014/408021.

Singh, T., Jyoti, K., Patnaik, A., Singh, A., Chauhan, R. and Chandel, S.S. (2017), "Biosynthesis, characterization and antibacterial activity of silver nanoparticles using an endophytic fungal supernatant of *Raphanus sativus*", *J. Gen. Eng. Biotechnol*., **15**(1), 31-39. https://doi.org/10.1016/j.jgeb.2017.04.005.

Sunkar, S. and Nachiyar, C.V. (2012), "Biogenesis of antibacterial silver nanoparticles using the endophytic bacterium *Bacillus cereus* isolated from *Garcinia xanthochymus*", *Asia. Pac. J. Tropical Biomed*., **2**(12), 953-959. https://doi.org/10.1016/S2221-1691(13)60006-4.

Tamura, K., Nei, M. and Kumar, S. (2004), "Prospects for inferring very large phylogenies by using the neighbor-joining method", *Proceedings of the National Academy of Sciences*, **101**(30), 11030-5. https://doi.org/10.1073/pnas.0404206101

Vicentin, R.P., Santos, J.V., Labory, C.R., Costa, A.M., Moreira, F.M. and Alves, E. (2018), "Tolerance to and accumulation of Cadmium, Copper, and Zinc by *Cupriavidus necator*", *Revista Brasileira de Ciência do Solo*, **42**. https://doi.org/10.1590/18069657rbcs20170080.

Wang, M., Li, H., Li, Y., Mo, F., Li, Z., Chai, R. and Wang, H. (2020), "Dispersibility and size control of silver nanoparticles with anti-algal potential based on coupling effects of polyvinylpyrrolidone and sodium tripolyphosphate", *Nanomaterials*, **10**(6), 1042. https://doi.org/10.3390/nano10061042.

White, T.J., Bruns, T., Lee, S.J. and Taylor, J. (1990), "Amplification and direct sequencing of fungal ribosomal RNA genes for phylogenetics", *PCR Protocols: A Guide to Methods and Applications*, **18**(1), 315-22.

Yildiz, Y., Okyay, T.O., Sen, B., Gezer, B., Kuzu, S., Savk, A., Demir, E., Dasdelen, Z., Sert, H. and Sen, F. (2017), "Highly monodisperse Pt/Rh nanoparticles confined in the graphene oxide for highly efficient and reusable sorbents for methylene blue removal from aqueous solutions", *Chem. Select*, **2**(2), 697-701. https://doi.org/10.1002/slct.201601608.

Zailani, A.H., Jada, S.M. and Wurochekke, U.A. (2010), "Antimicrobial activity of *Waltheria indica*", *J. Am. Sci*., **6**(12), 1591-1594.

Zhang, H.W., Song, Y.C. and Tan, R.X. (2006), "Biology and chemistry of endophytes", *Nat. Prod. Rep*., **23**(5), 753-771. https://doi.org/10.1039/B609472B.

Zongo, F., Ribuot, C., Boumendjel, A. and Guissou, I. (2013), "Botany, traditional uses, phytochemistry and pharmacology of *Waltheria indica* L. (syn. *Waltheria americana*): A review", *J. Ethnopharmacol*., **148**(1), 14-26. https://doi.org/10.1016/j.jep.2013.03.080.

CC